

# Technical Notes and Correspondence

## Extremum Seeking With Stochastic Perturbations

Chris Manzie and Miroslav Krstic

**Abstract**—Extremum seeking (ES) using deterministic periodic perturbations has been an effective method for non-model based real time optimization when only limited plant knowledge is available. However, periodicity can naturally lead to predictability which is undesirable in some tracking applications and unrepresentative of biological optimization processes such as bacterial chemotaxis. With this in mind, it is useful to investigate employing stochastic perturbations in the context of a typical ES architecture, and to compare the approach with existing stochastic optimization techniques. In this work, we show that convergence towards the extremum of a static map can be guaranteed with a stochastic ES algorithm, and quantify the behavior of a system with Gaussian-distributed perturbations at the extremum in terms of the ES constants and map parameters. We then examine the closed loop system when actuator dynamics are included, as the separation of time scales between the perturbation signal and plant dynamics recommended in periodic ES schemes cannot be guaranteed with stochastic perturbations. Consequently, we investigate how actuator dynamics influence the allowable range of ES parameters and necessitate changes in the closed loop structure. Finally simulation results are presented to demonstrate convergence and to validate predicted behavior about the extremum. For the sake of analogy with the classical methods of stochastic approximation, stochastic ES in this technical note is pursued in discrete time.

**Index Terms**—Extremum seeking (ES).

### I. INTRODUCTION

ALTHOUGH sinusoid-based extremum seeking (ES) was popular in the 1950s, the local stability results in [13] spawned renewed interest within the theoretical control community and several applied communities. The new developments included different classes of ES schemes [1], extensions to discrete time [4] and semi-global stability results [12]. As a consequence of these theoretical developments, numerous applications from engine calibration [8] to plasma control in Tokamaks [7] have been recently proposed.

Extremum seeking is a non-model based, real-time optimization algorithm that uses zero-mean perturbations to develop a gradient estimate. The gradient estimate is then used to shift the state variable towards the extremum. A common thread in the published ES literature to date is a reliance on periodic perturbations. The predictability associated with periodic perturbations can be disadvantageous for some tracking applications (where a vehicle navigated by a periodic extremum seeking algorithm can become a predictable target), while certain biological systems (such as bacterial chemotaxis) do not utilize periodicity in locating optima. Furthermore, if the system has high dimensionality, the orthogonality requirements on the elements of the

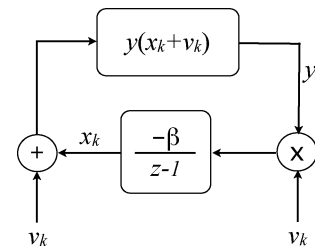


Fig. 1. First order ES system where  $x_k$  and  $v_k$  are the state of the system and perturbation at time  $k$ , and  $y(\cdot)$  is a static map.

periodic perturbation vector pose an implementation challenge. Stochastic perturbations may offer a potential solution to these problems.

The simplest sinusoidal ES architecture was proposed by Tan *et al.* in [12]. This structure differs from the earlier structures used in [13] by the removal of the washout filter prior to the state update, and is illustrated in discrete time form in Fig. 1. This first order scheme will be used as the base architecture in the initial discussions in this technical note, and allow the closed loop system in Fig. 1 to be expressed as the vector difference equation

$$x_{k+1} = x_k - \beta v_k y(x_k + v_k). \quad (1)$$

**Assumption 1.1:** The elements of the stochastic perturbation vector,  $v_k$ , are sequentially and mutually independent such that  $\mathbb{E}(v_k) = 0$ ,  $\mathbb{E}(v_{i,k}^2) = \sigma_i^2$  and  $\mathbb{E}(v_{i,k} v_{j,k}) = 0 \forall i \neq j$ . Further, it is also assumed that the p.d.f. of the perturbation vector is symmetric about its mean.

Of course, the concept of using stochastic perturbations in optimization is not new and a rich and mature field of stochastic approximation exists. Within this field there are some basic commonalities, fundamentally the optimization is implicitly or explicitly derived from the classical gradient descent law whereby updates to the state variable,  $x_k$ , of the form  $x_{k+1} = x_k - a_k(dy(x_k)/dx)$ , are used to find the state,  $x^*$ , minimizing the output  $y(x_k)$ . However since direct measurements of the gradient are usually unavailable for applications involving real systems, the optimization algorithms take the form of approximated gradient descent, i.e.  $x_{k+1} = x_k - a_k \hat{g}_k(x_k)$ , where  $\hat{g}_k(x_k)$  is the gradient estimate determined by the specific algorithm.

Stochastic approximation methods for estimating the gradient are often grouped into three basic classes—Finite Difference Stochastic Approximation (FDSA) [3], [5]; Random Direction Stochastic Approximation (RDSA) [6] and Simultaneous Perturbation Stochastic Approximation (SPSA) [9], [11].

In the FDSA algorithm, each element of the state vector is perturbed one at a time, and each element of the gradient vector is estimated according to  $\hat{g}_{i,k}(x_k) = (y(x_k + v_{i,k}) - y(x_k - v_{i,k}))/2v_{i,k}$  for  $i = 1 \dots N$ . While giving the best estimate of the gradient direction at the current point, this algorithm requires  $2N$  perturbations for every state update in an  $N$  dimensional system, and consequently is not well suited to fast implementation.

In the RDSA algorithm, all the elements of the state vector experience a perturbation at the same time but the effect on the output is averaged across all the elements of the gradient vector,  $\hat{g}_k(x_k) = \Delta_k(y(x_k + c_k \Delta_k) - y(x_k - c_k \Delta_k))/2c_k$ , where the elements of the

Manuscript received June 21, 2007; revised September 27, 2007. Current version published March 11, 2009. Recommended by Associate Editor J.-F. Zhang.

C. Manzie is with the Department of Mechanical Engineering, The University of Melbourne, Victoria 3010, Australia (e-mail: manziec@unimelb.edu.au).

M. Krstic is with the Department of Mechanical and Aerospace Engineering, University of California at San Diego, La Jolla, CA 92093 USA (e-mail: krstic@ucsd.edu).

Digital Object Identifier 10.1109/TAC.2008.2008320

perturbation vector  $\Delta_k = [\Delta_{1,k} \cdots \Delta_{n,k}]^T$  may have separate distributions. This approach guarantees a correct gradient traversal of the static surface being optimized, and requires only two measurements per update. Similarly, in the SPSA algorithm only two perturbations and measurements are used per update, however in this case the magnitude of the perturbation is used to normalize the gradient estimation in the direction of the perturbation, i.e.  $\hat{g}_{i,k}(x_k) = (y(x_k + c_k \Delta_k) - y(x_k - c_k \Delta_k)) / 2c_k \Delta_{i,k}$ .

The random variables used in RDSA and SPSA must satisfy certain conditions, although these are not identical in general and typically more limiting for the SPSA algorithm—e.g. RDSA can tolerate a perturbation  $\Delta_{i,k} = 0$  whereas SPSA clearly cannot. An important point is that both the RDSA and SPSA algorithms contain two perturbations in opposite directions, however a one-measurement version of SPSA was investigated in [10] and shown to be capable of locating the optimum of a static map, albeit typically not as quickly or as smoothly as the two measurement version of the algorithm. The one-measurement SPSA algorithm, with  $x_{k+1} = x_k - (a_k y(x_k + c_k \Delta_k) / c_k) [\Delta_{1,k}^{-1} \cdots \Delta_{N,k}^{-1}]^T$  represents the simplest form of stochastic approximation algorithm we are aware of, and represents a more suitable implementation for a dynamic system where the state may not remain constant between two successive perturbations. It is not surprising then that one-measurement SPSA shares some commonalities with the ES algorithm of (1), although they are not equivalent *except, just formally*, in two cases: 1) when  $x_k$  is a scalar and  $a_k = \beta(c_k \Delta_k)^2$  (which is not a choice that would normally be made in the stochastic approximation algorithms because  $a_k$  should be deterministic and go to zero as  $k$  goes to infinity); and 2) when  $x_k$  is a vector and each element of  $v_k$  is an unbiased Bernoulli-type variable from the set  $\{-1, +1\}$ . On the other hand, the appearance of the perturbation in the numerator of (1) is reminiscent of the RDSA state update, however, we do not consider classifying the stochastic ES as simply a one-measurement RDSA algorithm due to the common presence of a washout filter in the feedback loop when implementing ES. This modification has not been used with a stochastic RDSA algorithm previously.

A further important point is the stochastic approximation algorithms enforce  $c_k \rightarrow 0$ . Spall shows the bias in the gradient estimate is  $O(c_k^2)$  in Lemma 1 of [11], thus bias in the gradient estimate can be totally eliminated by  $c_k \rightarrow 0$ . While this may be acceptable for large dimensional static problems, it is restrictive for online optimization when the plant is subject to state disturbances, set point changes or drift in the optimum. Thus the stochastic ES approach will utilize a constant step size. A consequence of this is Proposition 1 of [11] cannot be used to show convergence of  $x_k$  to the extremum  $x^*$  for the stochastic ES algorithm.

## II. CONVERGENCE OF THE FIRST ORDER STOCHASTIC ES ALGORITHM

The convergence of the first order stochastic ES algorithm illustrated in Fig. 1 is addressed by finding the conditions for convergence of the averaged system, then showing the difference between the averaged and true systems are bounded almost surely in the limit  $k \rightarrow \infty$ .

*Assumption 2.1:* The output mapping is quadratic (at least locally), i.e.

$$y(x_k) = (x_k - x^*)^T A(x_k - x^*) + y_{\min} \quad (2)$$

where  $x^*$  and  $y_{\min}$  are unknown constants, and  $A = \text{diag}[A_1, A_2, \dots, A_n] \in \mathbb{R}^{n \times n}$ .

Without loss of generality, we further set  $x^* = 0$  as a simple change of variable  $x_k - x^* \mapsto x_k$  can be used to achieve this. Since the algorithm (1) contains an integrator, all uncertainty is thereby absorbed into

the initial condition,  $x_0$ . Consequently, in the remainder of this technical note all measures relating to the state  $x_k$  (e.g., mean and variance) refer to the deviation of the state from the minimising value,  $x_k - x^*$ . Note that the algorithm (as with all ES schemes) relies only on perturbation and output measurements: knowledge of  $x^*$  is not required for implementation.

### A. The Averaged System

The averaged system is obtained by taking the expectation of the closed loop system (1) under Assumption 2.1

$$\begin{aligned} \mathbb{E}(x_{k+1}) = \mathbb{E}(x_k) - \beta \mathbb{E} \left( v_k x_k^T A x_k \right) - \beta y_{\min} \mathbb{E}(v_k) \\ - \beta \mathbb{E} \left( 2v_k v_k^T A x_k \right) - \beta \mathbb{E} \left( v_k v_k^T A v_k \right). \end{aligned} \quad (3)$$

Since  $v_k$  and  $x_k$  are independent, from Assumption 1.1 it follows that  $\mathbb{E}(v_k x_k^T A x_k) = 0$ ;  $\mathbb{E}(v_k v_k^T A v_k) = 0$ ; and  $\mathbb{E}(v_k v_k^T A x_k) = \Sigma_d \mathbb{E}(x_k)$  where  $\Sigma_d = A \times \text{diag}[\sigma_1^2 \dots \sigma_N^2]$ . Thus (3) reduces to  $\mathbb{E}(x_{k+1}) = (I - 2\beta \Sigma_d) \mathbb{E}(x_k)$ .

*Remark 1:* Since  $\beta$  and  $\sigma_i^2$  are all positive, the state of the averaged system,  $\mathbb{E}(x_k)$ , is exponentially convergent to the origin if  $\beta < 0.5 / \max_i(A_i \sigma_i^2)$ .

*Theorem 1:* Given an initial condition  $x_0$ ,  $\beta < 0.5 / \max_i(A_i \sigma_i^2)$  can be chosen sufficiently small that for all  $\rho > 0$  there exists a constant  $C(\beta)$  such that the difference between the solution of the true system and the equilibrium of the averaged system obeys

$$\limsup_{k \rightarrow \infty} P(\|x_k\| > \rho) \leq C(\beta) \text{ where } C(\beta) \rightarrow 0 \text{ as } \beta \rightarrow 0. \quad (4)$$

*Proof:* The result follows from (2) and from Theorem 3, p44, in Benveniste *et al.* [2]. ■

## III. PREDICTION OF BEHAVIOR AT STEADY STATE FOR GAUSSIAN PERTURBATIONS

Since the step size,  $\beta$ , used in the ES algorithm is non-decreasing, unlike in the SPSA approach, there will be variations about the extremum of the mapping as  $k \rightarrow \infty$ . To investigate this behavior of the system, we consider the special case where  $v_{i,k}$  is a Gaussian sequence satisfying Assumption 1.1. Gaussian perturbations are not intended to represent an optimal perturbation sequence for all input-output maps, but to allow quantitative results to be presented utilising the known equalities  $\mathbb{E}(v_{i,k}^{2n+1}) = 0$ ,  $\mathbb{E}(v_{i,k}^4) = 3\sigma_i^4$  and  $\mathbb{E}(v_{i,k}^6) = 15\sigma_i^6$ . A similar analysis may be undertaken for other perturbations such as Bernoulli  $\{+1, -1\}$  distributed sequences using  $\mathbb{E}(v_{i,k}^{2n}) = 1$  and  $\mathbb{E}(v_{i,k}^{2n+1}) = 0$ .

### A. Scalar Case

We begin with the state update (1), which for a scalar system is given by

$$x_{k+1} = x_k - \beta f_k \quad (5)$$

$$\begin{aligned} \text{where } f_k = v_k y_k = A(v_k^3 + 2x_k v_k^2 + x_k^2 v_k) + v_k y_{\min} \\ = f_{0,k} + v_k y_{\min}. \end{aligned}$$

Note that  $f_{0,k}$  is the value of  $f_k$  if  $y_{\min} = 0$ , and is defined only to simplify some of the notational detail.

*Assumption 3.1:*  $\mathbb{E}(x_k^4) \geq \mathbb{E}(x_k^6) \geq \mathbb{E}(x_k^8) \forall k$ .

*Remark 2:* This assumption is clearly restrictive, though it is not unreasonable when  $x_0$ ,  $\sigma^2$  and  $\beta$  are small.

We now define  $\eta(\beta, \sigma, y_{\min}, A) = 4A\beta\sigma^2 - 18A^2\beta^2\sigma^4 - 2Ay_{\min}\beta^2\sigma^2$ ;  $\kappa(\beta, \sigma, A) = A^2\beta^2\sigma^2$ ;  $\delta(\beta, \sigma, y_{\min}, A) = 15A^2\beta^2\sigma^6 + 6A\beta^2y_{\min}\sigma^4 + \beta^2y_{\min}^2\sigma^2$ ;  $\lambda(\beta, \sigma, y_{\min}, A) =$

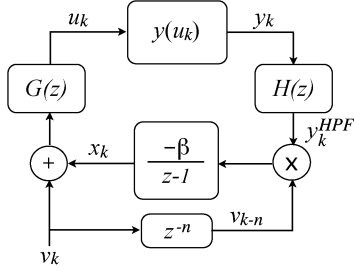


Fig. 2. Extremum seeking system with actuator,  $G(z)$ , and washout filter,  $H(z)$ . The relative degree of  $G(z)$  is  $n$ .

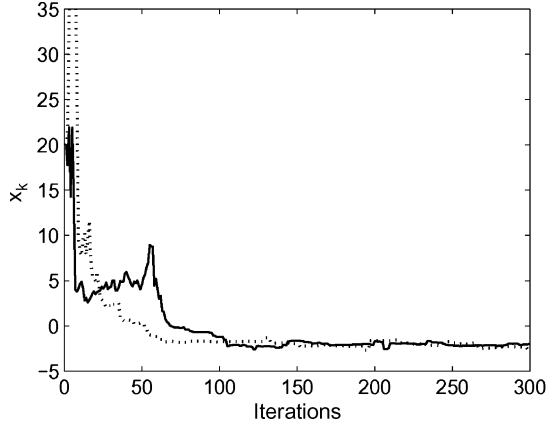


Fig. 3. Scalar simulation: convergence of  $x_k$  to extremum at  $x^* = -2$  for two different realizations of  $v_k$ .

$90A^2\beta^2\sigma^6 + 36Ay_{\min}\beta^2\sigma^4 + 6y_{\min}^2\beta^2\sigma^2$ ; and  $\gamma(\beta, \sigma, y_{\min}, A) = 8A\beta\sigma^2 - 108A^2\beta^2\sigma^4 - 12y_{\min}\beta^2\sigma^2$ .

**Assumption 3.2:** The eigenvalues of the matrix  $\begin{bmatrix} 1 - \eta & \kappa \\ \lambda & 1 - \gamma \end{bmatrix}$  are inside the unit disc.

**Theorem 2:** Given Assumptions 2.1, 3.1 and 3.2 and Gaussian perturbations satisfying Assumption 1.1, the variance in the state,  $\mathbb{E}(x_k^2) \rightarrow (\delta\gamma/(\eta\gamma - \kappa\lambda)) + O(\beta^2)$  as  $k \rightarrow \infty$ .

**Remark 3:** For small  $\beta$ , we note that  $\delta\gamma = O(\beta^3)$ ,  $\kappa\lambda = O(\beta^4)$  and  $\eta\gamma = O(\beta^2)$ . Hence it follows from Theorem 2 that  $\mathbb{E}(x_k^2) = O(\beta) \rightarrow 0$  as  $\beta \rightarrow 0$ .

**Proof of theorem 2:** By squaring (5) and taking the expectation it follows that:

$$\mathbb{E}(x_{k+1}^2) = \mathbb{E}(x_k^2 - 2\beta f_{0,k}x_k + \beta^2 f_{0,k}^2) + 2\mathbb{E}(\beta^2 y_{\min} f_{0,k} v_k) + \mathbb{E}(\beta^2 y_{\min}^2 v_k^2) - 2\mathbb{E}(\beta y_{\min} v_k x_k). \quad (6)$$

The first term on the right hand side of (6) is the variance for  $y_{\min} = 0$ , and is given by  $\mathbb{E}(x_k^2 - 2\beta f_{0,k}x_k + \beta^2 f_{0,k}^2) = (1 - 4A\beta\sigma^2 + 18A^2\beta^2\sigma^4)\mathbb{E}(x_k^2) + A^2\beta^2\sigma^2\mathbb{E}(x_k^4) + 15A^2\beta^2\sigma^6$ . The remaining terms in (6) are  $2\mathbb{E}(\beta^2 y_{\min} f_{0,k} v_k) = 2A\beta^2 y_{\min}(3\sigma^4 + \sigma^2\mathbb{E}(x_k^2))$ ;  $\mathbb{E}(\beta^2 y_{\min}^2 v_k^2) = \beta^2 y_{\min}^2 \sigma^2$  and  $2\mathbb{E}(\beta y_{\min} v_k x_k) = 0$ . Consequently, it follows that the variance in  $x_k$  is given by:

$$\mathbb{E}(x_{k+1}^2) = (1 - \eta)\mathbb{E}(x_k^2) + \kappa\mathbb{E}(x_k^4) + \delta. \quad (7)$$

Similarly, it can be shown  $\mathbb{E}(x_{k+1}^4) = O(\beta^4)\mathbb{E}(x_k^8) - O(\beta^3)\mathbb{E}(x_k^6) + [1 - 8A\beta\sigma^2 + 108A^2\beta^2\sigma^4 + 12Ay_{\min}\beta^2\sigma^2 + O(\beta^3)]\mathbb{E}(x_k^4) + [90A^2\beta^2\sigma^6 + 36y_{\min}A\beta^2\sigma^4 + 6\beta^2 y_{\min}^2\sigma^2 + O(\beta^3)]\mathbb{E}(x_k^2) + O(\beta^4)$ . Applying Assumption 3.1 to this expectation leads to

$$\mathbb{E}(x_{k+1}^4) \leq (\lambda + O(\beta^3))\mathbb{E}(x_k^2)$$

$$+ (1 - \gamma + O(\beta^3))\mathbb{E}(x_k^4) + O(\beta^4). \quad (8)$$

Equation (7) and the upper limit of (8) represent a (weakly) coupled set of equations. Given Assumption 3.2, the  $\mathbb{E}(x_k^2)$  sequence will approach the result of Theorem 2 as  $k \rightarrow \infty$ . ■

**Theorem 3:** Given the system satisfies Assumptions 2.1, 3.1 and 3.2 and uses Gaussian perturbations satisfying Assumption 1.1, then as  $k \rightarrow \infty$

$$\begin{aligned} \mathbb{E}(y - y_{\min}) &\rightarrow A \left( \frac{\delta\gamma}{\eta\gamma - \kappa\lambda} + \sigma^2 \right) \\ &\rightarrow A\sigma^2 \text{ as } \beta \rightarrow 0^+ \\ \text{var}(y_k - y_{\min}) &\rightarrow A^2 \left( \frac{(\lambda + 6\sigma^2\gamma)\delta}{\eta\gamma - \kappa\lambda} + 3\sigma^4 \right) \\ &\quad - A^2 \left( \frac{\delta\gamma}{\eta\gamma - \kappa\lambda} + \sigma^2 \right)^2 \\ &\rightarrow 2A^2\sigma^4 \text{ as } \beta \rightarrow 0^+. \end{aligned} \quad (9)$$

### B. Vector Case

The asymptotic value of the covariance matrix of  $x_k$  can be derived for the non-scalar case. We begin by adjusting Assumptions 3.1 and 3.2 as follows:

**Assumption 3.3:**  $\mathbb{E}(x_{i,k}^2) \geq \mathbb{E}(x_{i,k}^4)$  and  $\mathbb{E}(x_{i,k}^2) \geq \mathbb{E}(x_{i,k}^2 x_{j,k}^2)$   $\forall i, j, k$

**Remark 4:** Assumption 3.3 is more restrictive than the equivalent assumption for the scalar case (Assumption 3.1). This will allow for a concise formulation of the results when dealing with the non-scalar state than would otherwise be the case.

We define  $\bar{\delta}_i(\beta, \sigma, y_{\min}, A) = 15\beta^2 A_i^2 \sigma_i^6 + 6\beta^2 A_i y_{\min} \sigma_i^4 + \beta^2 \sigma_i^2 y_{\min}^2 + \beta^2 \sigma_i^2 \sum_{j=1, j \neq i}^N (3A_j \sigma_j^4 + 2y_{\min} A_j \sigma_j^2 + 6A_j^2 \sigma_j^2 \sigma_i^2) + 2\beta^2 \sigma_i^2 \sum_{j=1, j \neq i}^N \sum_{k=1, k \neq i}^{k-1} A_j A_k \sigma_j^2 \sigma_k^2$ ;  $\bar{\eta}_i(\beta, \sigma, y_{\min}, A) = 4\beta A_i \sigma_i^2 - 18\beta^2 A_i^2 \sigma_i^4 - 2\beta^2 \sigma_i^2 \sum_{j=1, j \neq i}^N A_j \sigma_j^2 - 2\beta^2 \sigma_i^2 A_i y_{\min}$ ;  $\bar{\alpha}_{ij}(\beta, \sigma, y_{\min}, A) = 2\beta^2 y_{\min} A_j \sigma_i^2 + 5\beta^2 A_j^2 \sigma_j^2 + 6\beta^2 A_j^2 \sigma_i^2 + 2\beta^2 \sigma_i^2 A_j \sum_{k=1, k \neq i}^N \sigma_k^2$ ;  $\bar{\Gamma}_{ii} = \bar{\eta}_i$  and  $\bar{\Gamma}_{ij} = -\bar{\alpha}_{ij}$ ; and  $[\mu_1 \dots \mu_N]^T = \bar{\Gamma}^{-1}[\bar{\delta}_1 \dots \bar{\delta}_N]^T$ .

**Assumption 3.4:** The eigenvalues of the matrix  $I - \bar{\Gamma}$  are inside the unit disc.

**Theorem 4:** Given Assumptions 2.1, 3.3 and 3.4 and using Gaussian perturbations satisfying Assumption 1.1 the covariance matrix  $\mathbb{E}(x_k x_k^T) \rightarrow \text{diag}[\mu_1, \dots, \mu_N] + O(\beta)I$  as  $k \rightarrow \infty$ .

**Remark 5:** Note that for the case  $N = 1$  the covariance matrix limit reduces to

$$\begin{aligned} \text{cov}(x_k) &\rightarrow \frac{15\beta^2 A^2 \sigma^6 + 6\beta^2 A y_{\min} \sigma^4 + \beta^2 \sigma^2 y_{\min}^2}{4\beta A \sigma^2 - 18\beta^2 A^2 \sigma^4 - 2\beta^2 \sigma^2 A y_{\min}} + O(\beta) \\ &= \frac{\delta}{\eta} + O(\beta) \end{aligned} \quad (11)$$

as expected from (7) if Assumption 3.1 is replaced with Assumption 3.3.

**Proof of theorem 4:** From Assumption 1.1 the off diagonal terms ( $i \neq j$ ) in the covariance matrix are  $\mathbb{E}(x_{i,k+1} x_{j,k+1}) = \mathbb{E}(x_{i,k} x_{j,k}) - \beta \mathbb{E}(x_{i,k} v_{j,k} y_k) - \beta \mathbb{E}(x_{j,k} v_{i,k} y_k)$ . Given Assumption 2.1 for each  $i$  and  $j$  it follows that  $\mathbb{E}(x_{i,k} v_{j,k} y_k) = 2\sigma_j^2 A_j \mathbb{E}(x_{i,k} x_{j,k})$ . The off-diagonal terms in the covariance matrix subsequently become  $\mathbb{E}(x_{i,k+1} x_{j,k+1}) = \mathbb{E}(x_{i,k} x_{j,k}) [1 - 2A_j \beta \sigma_j^2 - 2A_i \beta \sigma_i^2]$ . For  $\beta < (1/4 \max_i(A_i \sigma_i^2))$  (which follows from the small  $\beta$  conditions of Assumptions 3.3–3.4) all off-diagonal terms are convergent to zero as  $k \rightarrow \infty$ . The diagonal terms in the covariance matrix can now be addressed by substituting  $i = j$  into  $\mathbb{E}(x_{i,k+1}^2) = \mathbb{E}(x_{i,k}^2) - 2\beta \mathbb{E}(x_{i,k} v_{i,k} y_k) + \beta^2 \mathbb{E}(v_{i,k}^2 y_k^2)$ . The final

TABLE I  
 COMPARISON OF PREDICTED AND SIMULATION RESULTS FOR SCALAR SYSTEM

$(A, \beta, \sigma^2, y_{\min})$	Predicted $\mathbb{E}(x^2)$	Sample $\mathbb{E}(x^2)$	Sample $\mathbb{E}(x^4)$	Sample $\mathbb{E}(x^6)$	Sample $\mathbb{E}(x^8)$	Predicted $\text{var}(y)$	Sample $\text{var}(y)$
$(2, 10^{-2}, 1, 0)$	0.082	0.084	0.04	0.03	0.03	9.4	9.4
$(1, 10^{-2}, 1, 0)$	0.039	0.038	$4.7 \times 10^{-3}$	$9.6 \times 10^{-4}$	$2.6 \times 10^{-4}$	2.2	2.2
$(1, 10^{-3}, 1, 0)$	$3.8 \times 10^{-3}$	$4.0 \times 10^{-3}$	$4.6 \times 10^{-5}$	$8.2 \times 10^{-7}$	$1.7 \times 10^{-8}$	2.02	2.04
$(1, 10^{-3}, 0.25, 0)$	$3.6 \times 10^{-6}$	$2.4 \times 10^{-6}$	$4.0 \times 10^{-10}$	$2.6 \times 10^{-14}$	$8.8 \times 10^{-19}$	$7.8 \times 10^{-3}$	$7.8 \times 10^{-3}$
$(2, 10^{-2}, 0.5, 2)$	0.016	0.017	$1.2 \times 10^{-5}$	$1.2 \times 10^{-7}$	$1.6 \times 10^{-9}$	0.57	0.56

term on the right hand side of this equation can be expanded using Assumption 2.1

$$\begin{aligned}
 \mathbb{E}(v_{i,k}^2 y_k^2) &= \mathbb{E}\left(v_{i,k}^2 \left((x_k + v_k)^T A(x_k + v_k) + y_{\min}\right)^2\right) \\
 &= \mathbb{E}\left(v_{i,k}^2 \left(\sum_{j=1}^N A_j (x_{j,k}^2 + v_{j,k}^2)\right)^2\right) \\
 &\quad + \mathbb{E}\left(4v_{i,k}^2 \left(\sum_{j=1}^N A_j x_{j,k} v_{j,k}\right)\right) + \mathbb{E}(v_{i,k}^2 y_{\min}^2) \\
 &\quad + \mathbb{E}\left(2v_{i,k}^2 y_{\min} \sum_{j=1}^N A_j (x_{j,k}^2 + v_{j,k}^2)\right). \quad (12)
 \end{aligned}$$

Note the subscript “k” applies to every term on the right hand side of (12) and so for brevity these subscripts will be omitted. Treating each term in (12) individually leads to the following identities:

$$\begin{aligned}
 &\mathbb{E}\left(v_i^2 \left(\sum_{j=1}^N A_j (x_j^2 + v_j^2)\right)^2\right) \\
 &= 2\sigma_i^2 \sum_{\substack{j=1 \\ j \neq i}}^N \sum_{\substack{k=1 \\ k \neq i}}^{j-1} A_j A_k \left(\mathbb{E}(x_j^2 x_k^2) + \sigma_j^2 \mathbb{E}(x_k^2)\right) \\
 &\quad + \sigma_k^2 \mathbb{E}(x_j^2) + \sigma_j^2 \sigma_k^2 \\
 &\quad + A_i^2 (15\sigma_i^6 + 6\sigma_i^4 \mathbb{E}(x_i^2) + \sigma_i^2 \mathbb{E}(x_i^4)) \\
 &\quad + \sigma_i^2 \sum_{\substack{j=1 \\ j \neq i}}^N A_j^2 (3\sigma_j^4 + \sigma_j^2 \mathbb{E}(x_j^2) + \mathbb{E}(x_j^4)) \\
 &\quad + \sum_{\substack{j=1 \\ j \neq i}}^N A_j^2 (2\sigma_i^2 \mathbb{E}(x_i^2 x_j^2) + 6\sigma_i^4 \sigma_j^2 \\
 &\quad \quad + 6\sigma_i^2 \mathbb{E}(x_j^2) + 2\sigma_i^2 \sigma_j^2 \mathbb{E}(x_i^2)) \quad (13)
 \end{aligned}$$

$$\begin{aligned}
 &\mathbb{E}\left(4v_i^2 \left(\sum_{j=1}^N A_j x_j v_j\right)^2\right) \\
 &= 12A_i^2 \sigma_i^4 \mathbb{E}(x_i^2) + 4\sigma_i^2 \sum_{\substack{j=1 \\ j \neq i}}^N A_j^2 \sigma_j^2 \mathbb{E}(x_j^2) \\
 &\quad + 8 \sum_{\substack{j=1 \\ j \neq i}}^N \sum_{\substack{k=1 \\ k \neq i}}^{j-1} A_i A_j \mathbb{E}(x_j x_k) \mathbb{E}(v_i^2 v_j^2 v_k^2) \quad (14)
 \end{aligned}$$

$$\mathbb{E}\left(2v_i^2 y_{\min} \sum_{j=1}^N A_j (x_j^2 + v_j^2)\right)$$

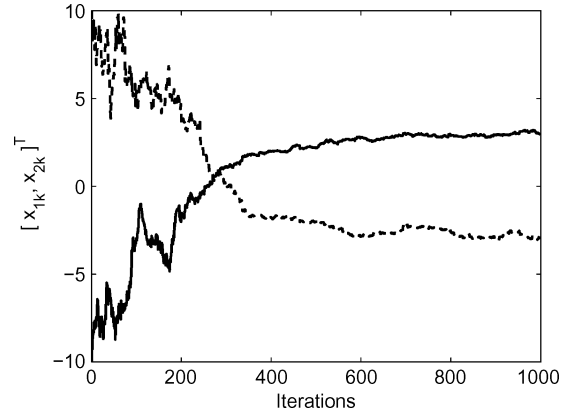


Fig. 4. Vector simulation: convergence of  $x_k$  to extremum at  $x^* = [3, -3]^T$  of (solid)  $x_{1,k}$  and (dashed)  $x_{2,k}$ .

 TABLE II  
 COMPARISON OF PREDICTED AND SIMULATION COVARIANCES

Map constants $A, y_{\min}$	ES constants $\beta \times 10^3, \sigma^2$	Predicted $\text{cov}(x) \times 10^2$	Sample $\text{cov}(x) \times 10^2$
$\begin{bmatrix} 3 & 0 \\ 0 & 2 \end{bmatrix}, 10$	$1, \begin{bmatrix} 1 \\ 2 \end{bmatrix}$	$\begin{bmatrix} 4.3 & 0 \\ 0 & 8.2 \end{bmatrix}$	$\begin{bmatrix} 5.1 & -0.1 \\ -0.1 & 8.1 \end{bmatrix}$
$\begin{bmatrix} 3 & 0 \\ 0 & 2 \end{bmatrix}, 0$	$1, \begin{bmatrix} 1 \\ 1 \end{bmatrix}$	$\begin{bmatrix} 1.2 & 0 \\ 0 & 0.9 \end{bmatrix}$	$\begin{bmatrix} 1.1 & -0.1 \\ -0.1 & 0.9 \end{bmatrix}$
$\begin{bmatrix} 1 & 0 \\ 0 & 1 \end{bmatrix}, 0$	$5, \begin{bmatrix} 0.5 \\ 2 \end{bmatrix}$	$\begin{bmatrix} 1.8 & 0 \\ 0 & 7.9 \end{bmatrix}$	$\begin{bmatrix} 2.7 & 0.1 \\ 0.1 & 8.7 \end{bmatrix}$

$$\begin{aligned}
 &= 2y_{\min} \sigma_i^2 \sum_{j=1}^N A_j \mathbb{E}(x_j^2) \\
 &\quad + 2y_{\min} \sigma_i^2 \sum_{\substack{j=1 \\ j \neq i}}^N A_j \sigma_j^2 + 6y_{\min} A_i \sigma_i^4 \quad (15)
 \end{aligned}$$

$$\mathbb{E}(v_i^2 y_{\min}^2) = \sigma_i^2 y_{\min}^2. \quad (16)$$

Assumption 3.3 allows (13) and (14) to be simplified. The subsequent equations, along with (15) and (16) can then be substituted into (12) to yield the coupled system  $\mathbb{E}[x_1^2 \dots x_N^2]_{k+1}^T = \bar{\Gamma} \mathbb{E}[x_1^2 \dots x_N^2]_k^T + [\bar{\delta}_1 \dots \bar{\delta}_N]^T$ . The result of Theorem 4 now follows directly when Assumption 3.4 is satisfied. ■

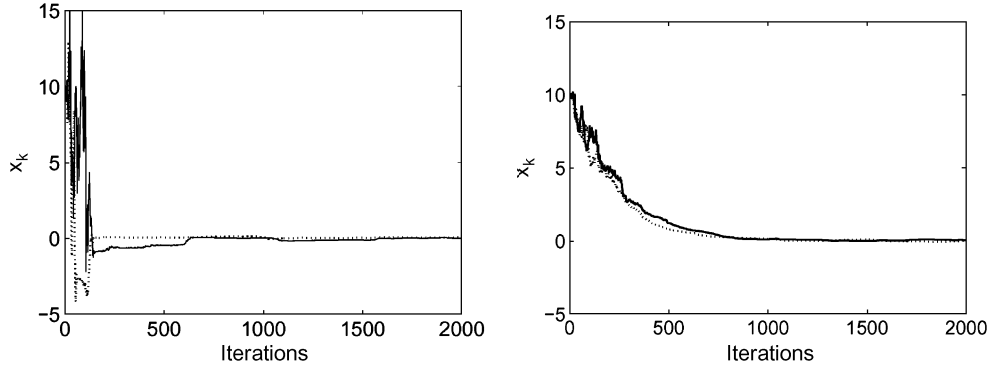


Fig. 5. Two stochastic iterations (left) without and (right) with washout filter for a scalar plant with slow dynamics.

**Theorem 5:** Given the system satisfies Assumptions 2.1, 3.3 and 3.4 and uses Gaussian perturbations satisfying Assumption 1.1, then  $\mathbb{E}(y_k - y_{min}) \rightarrow \sum_{i=1}^N A_i \sigma_i^2$  as  $\beta \rightarrow 0^+$  and  $k \rightarrow \infty$ .

**Remark 6:** Theorems 2–5 allow some general design guidelines to be proposed for the stochastic ES algorithm if some knowledge about the mapping is available. First, the variances of the perturbation vector should be chosen to maintain approximately equal  $A_i \sigma_i^2$  products to prevent one dimension dominating the output bias. The value of  $\beta$  should then be chosen to provide the desired balance between the rate of convergence and state covariance of the system.

#### IV. INCLUSION OF PLANT DYNAMICS AND WASHOUT FILTERS

The first order ES system discussed in Sections II and III is capable of locating the extremum of a static map, but in many engineering applications the plant dynamics must be considered in the analysis of the closed loop system. In the deterministic ES approaches of [13] the design procedure involves selecting the perturbation frequency to be of a time scale slower than the plant dynamics—however if the only requirement on the stochastic perturbations are Assumption 1.1 this time scale separation cannot be guaranteed. The closed loop ES system is modified by delaying the demodulating perturbation to allow convergence to the extremum for some range of  $\beta$  in the presence of a general actuator model,  $G(z)$ , of relative degree  $n$  and washout filter  $H(z)$ . The actuator dynamics require the introduction of an additional variable,  $u_k$ , to represent the input to the static map, while  $x_k$  represents the state of the ES scheme as before. The complete closed loop structure is illustrated in Fig. 2.

For brevity, the analysis in this section will restrict discussion to a stable, first-order linear actuator model,  $G(z) = W(z)/U(z) = b/(z - a)$  (i.e.  $n = 1$ ) to illustrate how the inclusion of actuator dynamics in the system effects the allowable range of  $\beta$  for convergence of the averaged system. Furthermore, while various possible washout filter designs are possible, we restrict our discussion to a filter of the form  $H(z) = Y^{HPPF}(z)/Y(z) = (z - 1)/(z + h)$ .

The state equations for this system are  $x_{k+1} = x_k - \beta v_{k-1} y_k^{HPPF}$ ,  $u_{k+1} = a u_k + b(x_k + v_k)$  and  $y_k^{HPPF} = -h y_{k-1}^{HPPF} + y_k - y_{k-1}$ . A new state variable  $e_k = ((h + 1)/(z + h)) y_k - y_{min}$  is proposed, leading to the reformulated system equations  $x_{k+1} = x_k - \beta v_{k-1} (y_k - e_k - y_{min})$ ,  $e_{k+1} = -h e_k + (h + 1) y_k - (h + 1) y_{min}$  and  $u_{k+1} = a u_k + b(x_k + v_k)$ .

Defining  $\eta_k = u_k - b(x_{k-1} + v_{k-1}) = a u_{k-1}$  leads to the difference equation  $x_{k+1} = x_k - \beta v_{k-1} [A(\eta_k - b x_{k-1})^2 + 2bA(\eta_k + b x_{k-1})v_{k-1} + Ab^2 v_{k-1}^2 + y_{min}]$ .

Now taking the expectation of this system and applying Assumption 1.1 leads to  $\mathbb{E}(\eta_{k+1}) = a\mathbb{E}(\eta_k) + ab\mathbb{E}(x_{k-1})$  and  $\mathbb{E}(x_{k+1}) = \mathbb{E}(x_k) - 2A\beta b\sigma^2(\mathbb{E}(\eta_k) + b\mathbb{E}(x_{k-1}))$ . Incrementing the latter equation and substituting the former yields the result  $\mathbb{E}(x_{k+2}) = \mathbb{E}(x_{k+1}) - 2A\beta b^2\sigma^2\mathbb{E}(x_k) + a\mathbb{E}(x_{k+1}) - a\mathbb{E}(x_k)$ .

**Remark 7:** The averaged system containing actuator dynamics and a washout filter will be stable if the poles of the equation  $z^2 - (1 + a)z + (a + 2A\beta b^2\sigma^2)$  lie inside the unit circle. From the root locus  $1 + \beta(2b^2\sigma^2/(z - 1)(z - a))$  it is clear that as  $a$  increases the maximum value of  $\beta$  for closed loop stability of the averaged system will decrease monotonically. The pole of the washout filter does not affect the stability of the averaged system and stability of the true system follows from Theorem 1.

**Remark 8:** The equilibrium point of the averaged system is  $\mathbb{E}[x, \eta, e]^{eq} = [0, 0, Ab^2\sigma^2]$ .

#### V. SIMULATION RESULTS

A scalar state and output mapping  $y_k = 2(x_k + 2)^2$  are considered. The initial value of the state is set to  $x_0 = 20$ , the ES update parameter  $\beta = 10^{-2}$  and  $N(0, 1)$  perturbations are used. Fig. 3 illustrates convergence to the extremum using two different realizations of the perturbation sequence,  $v_k$ . The sample variances were also found for single runs using different ES parameter values and compared to theoretical predicted values. The results are shown in Table I, and exhibit good correlation between the theory and experiment, as well as showing Assumption 3.1 holds. A two dimensional input-output mapping given by  $y_k = 3(x_{1,k} - 3)^2 + 2(x_{2,k} + 3)^2 + 10$  is then considered with the state is initialized to  $x_0 = [-10, 10]^T$ . The ES parameters were set to  $\beta = 10^{-3}$  and  $[\sigma_1^2, \sigma_2^2]^T = [1, 2]^T$ . The convergence in the states for one perturbation sequence is shown in Fig. 4. Table II shows good agreement between the simulated and predicted results for a range of ES parameters and maps.

Finally, slow actuator dynamics described by  $G(z) = 1/(z - 0.95)$  are included prior to the quadratic mapping  $y(u) = u^2$ . The ES parameters were set to  $\sigma^2 = 1$  and  $\beta = 10^{-4}$ , and the initial condition of the closed loop system was  $x_0 = 10$ . The behavior of the system for two separate iterations of  $v_k$  is shown in Fig. 5, with and without the inclusion of a washout filter  $H(z) = (z - 1)/(z + 0.2)$ . It is clear that the inclusion of the washout filter slows down convergence but increases the smoothness. This balance can be shifted by appropriately varying  $\beta$  and  $h$ .

#### VI. FURTHER WORK

Future areas for investigation include continuous time results, investigating the behavior of the full system with a time varying extremum and with different input-output mappings.

#### REFERENCES

- [1] K. B. Ariyur and M. Krstic, *Real Time Optimization by Extremum Seeking Control*. New York: Wiley, 2003.
- [2] A. Benveniste, M. Metivier, and P. Priouret, *Adaptive Algorithms and Stochastic Approximations*. New York: Springer-Verlag, 1990.

- [3] J. Blum, "Multidimensional stochastic approximation methods," *Annals Math. Stat.*, vol. 25, pp. 737–744, 1954.
- [4] J.-Y. Choi, M. Krstic, K. B. Ariyur, and J. S. Lee, "Extremum seeking control for discrete time systems," *IEEE Trans. Automat. Control*, vol. 47, no. 2, pp. 318–323, Feb. 2002.
- [5] J. Kiefer and J. Wolfowitz, "Stochastic estimation of the maximum of a regression function," *Annals Math. Stat.*, vol. 23, pp. 462–466, 1952.
- [6] H. Kushner and D. Clark, *Stochastic Approximation Methods for Constrained and Unconstrained Systems*. New York: Springer, 1978.
- [7] Y. Ou, C. Xu, E. Schuster, T. Luce, J. R. Ferron, and M. Walker, "Extremum-seeking finite-time optimal control of plasma current profile at the DIII-D Tokamak," in *Proc. Amer. Control Conf.*, Jul. 11–13, 2007, pp. 4015–4020.
- [8] D. Popovic, M. Jankovic, S. Magner, and A. Teel, "Extremum seeking methods for optimization of variable cam timing engine operation," *IEEE Trans. Control Syst. Technol.*, vol. 14, no. 3, pp. 398–407, May 2006.
- [9] J. Spall, "Multivariate stochastic approximation using a simultaneous perturbation gradient approximation," *IEEE Trans. Automat. Control*, vol. 37, no. 3, pp. 332–341, Mar. 1992.
- [10] J. Spall, "A one-measurement form of simultaneous perturbation stochastic approximation," *Automatica*, vol. 33, pp. 109–112, 1997.
- [11] J. Spall, "Implementation of the simultaneous perturbation algorithm for stochastic optimization," *IEEE Trans. Aerosp. Electron. Syst.*, vol. 3, no. 3, pp. 817–823, Jul. 1998.
- [12] Y. Tan, D. Netic, and I. Mareels, "On non-local stability properties of extremum seeking control," *Automatica*, vol. 42, pp. 889–903, 2006.
- [13] H.-H. Wang and M. Krstic, "Extremum seeking for limit cycle minimization," *IEEE Trans. Automat. Control*, vol. 45, no. 12, pp. 2432–2437, Dec. 2000.

## Controllability of Spacecraft Attitude Using Control Moment Gyroscopes

Sanjay P. Bhat and Pawan K. Tiwari

**Abstract**—This technical note describes an application of nonlinear controllability theory to the problem of spacecraft attitude control using control moment gyroscopes (CMGs). Nonlinear controllability theory is used to show that a spacecraft carrying one or more CMGs is controllable on every angular momentum level set in spite of the presence of singular CMG configurations, that is, given any two states having the same angular momentum, any one of them can be reached from the other using suitably chosen motions of the CMG gimbals. This result is used to obtain sufficient conditions on the momentum volume of the CMG array that guarantee the existence of gimbal motions which steer the spacecraft to a desired spin state or rest attitude.

**Index Terms**—Attitude control, controllability, control moment gyroscopes.

### I. INTRODUCTION

MOMENTUM exchange devices such as reaction wheels and control moment gyroscopes (CMGs) form an important class of torque actuators for spacecraft attitude control. Unlike mass expul-

Manuscript received June 18, 2007; revised May 18, 2008. Current version published March 11, 2009. This work was supported in part by the Indian Space Research Organization under its RESPOND program. This technical note appeared in part in the Proceedings of the American Control Conference, 2006. Recommended by Associate Editor F. Bullo.

S. P. Bhat is with the Department of Aerospace Engineering, Indian Institute of Technology Bombay, Powai, Mumbai-400076, India (e-mail: bhat@aero.iitb.ac.in).

P. K. Tiwari is with the Directorate of Tactical Missile Systems, Defense Research and Development Laboratory, Kanchanbagh, Hyderabad 500058, India (e-mail: tiwaripawan1@rediffmail.com).

Digital Object Identifier 10.1109/TAC.2008.2008324

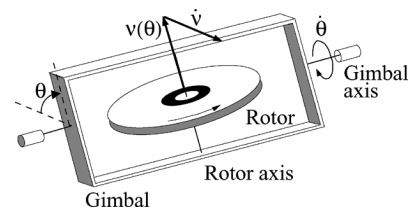


Fig. 1. Schematic of a SGCMG.

sion devices which alter the total angular momentum of the spacecraft, momentum exchange devices operate by changing the distribution of the angular momentum inside the spacecraft. Momentum exchange devices typically consist of spinning rotors which exchange momentum with the rest of the spacecraft through mutual interaction torques that either change the speed of rotation as in reaction wheels, or change the orientation of the spin axis as in CMGs, or change both as in variable speed CMGs.

CMGs are capable of producing significant torques and can handle large quantities of momentum over long periods of time. Consequently, CMGs are preferred in precision pointing applications and in momentum management of large, long-duration spacecraft. See, for instance, [1].

A CMG comprises of a rapidly spinning rotor mounted on one or two gimbals, and is accordingly called a *single gimbal CMG (SGCMG)* or a *double gimbal CMG*. Fig. 1 below shows a schematic of a SGCMG. The rotor spins at a constant rate about the rotor axis which is fixed to the gimbal. The gimbal itself can be rotated about the gimbal axis which is fixed in the spacecraft frame. The angular momentum vector  $\nu$  of the CMG rotor is a function of the gimbal angle  $\theta$ , but has a constant magnitude that depends on the rotor speed and inertia. Any rotation of the gimbal causes a change in the angular momentum vector of the CMG, and gives rise to an equal and opposite change in the angular momentum of the spacecraft. The control torque acting on the spacecraft is thus equal and opposite to the rate of change  $\dot{\nu}$  of the CMG angular momentum, and depends on the constant magnitude of  $\nu$  as well as the gimbal rotation rate  $\dot{\theta}$ . It is clear from the figure that the rotor angular momentum has a constant magnitude, and is constrained to rotate on a circle in a plane normal to the gimbal axis. Consequently, the rate of change of angular momentum  $\dot{\nu}$  at any instant is orthogonal to the angular momentum  $\nu$  and the gimbal axis. Hence, a SGCMG cannot produce torques in all directions.

In order to obtain torques along three independent directions, as well as for redundancy, CMGs are used in arrays consisting of multiple CMGs. Unfortunately, every CMG array possesses *singular configurations* [2]. For each singular configuration, there exists a singular direction along which the CMG array is unable to produce torque. More precisely, the mapping from gimbal angle rates to output torque becomes singular at singular configurations [3]. Fig. 2 shows a singular configuration for a system of four CMGs arranged in a pyramid array. The arrows  $\nu_1, \nu_2, \nu_3$  and  $\nu_4$  represent the angular momentum vectors of the individual CMGs. Each of these vectors is constrained to rotate in the plane of the pyramid face containing it. The dashed-dotted lines are normal to the pyramid faces, and represent the gimbal axes of the four CMGs. In the CMG configuration shown in Fig. 2,  $\nu_1$  and  $\nu_3$  are in the  $XZ$  plane, while  $\nu_2$  and  $\nu_4$  are parallel to the  $X$ -axis. The gimbal rates  $\dot{\theta}_1$  and  $\dot{\theta}_3$  give rise to instantaneous angular momentum rates  $\dot{\nu}_1$  and  $\dot{\nu}_3$  along the  $Y$ -axis. Similarly, the gimbal rates  $\dot{\theta}_2$  and  $\dot{\theta}_4$  give rise to instantaneous angular momentum rates  $\dot{\nu}_2$  and  $\dot{\nu}_4$  in the  $YZ$  plane. Thus, in the configuration shown, no combination of gimbal rates can produce a torque in the  $X$ -direction and hence, the configuration shown is a singular configuration with its singular direction along the  $X$ -axis.